ISSN 0208-7774 TRIBOLOGIA 2/2018 p. 139–151

Krzysztof WIERZCHOLSKI[*], Andrzej MISZCZAK[**]

IMPACT OF ADHESION AND VISCOSITY FORCES ON FRICTION VARIATIONS IN BIO-TRIBOLOGICAL SYSTEMS

WPŁYW SIŁ ADHEZJI I LEPKOŚCI NA ZMIANY SIŁ TARCIA W UKŁADACH BIOTRIBOLOGICZNYCH

Key words: bio-hydrodynamic lubrication, physiology fluids, viscosity, wettability, hydrogen ion concentration, friction forces, friction coefficients.

Abstract

The classical theory of lubrication holds that the lubricant dynamic viscosity increments cause the increments of hydrodynamic pressure, as well as friction forces and wear. In the case of high values of hydrodynamic pressure, it very often has a significant impact on the friction coefficient. New achievements in the field of micro-and nano-tribology provide for new hypotheses on the decrements and increments of the friction coefficient in the case of the lubricant viscosity increments. Experimental investigations have shown that, even in the case of decrements of the friction coefficient with the lubricant viscosity increments, such decrements are very often lower than simultaneous hydrodynamic pressure increments which results in the friction force increments with the lubricant viscosity increments.

In biological friction nods, we can observe a varied impact of the biological lubricant viscosity on the friction force and friction coefficient values. The abovementioned impact is caused by the adhesion and cohesion forces occurring between the biological fluid particles flowing around the phospholipid bilayer on the superficial layer of the cartilage with varied wettability and hydrogen ion concentration. The wettability (We) and power hydrogen ion concentration (pH) have a significant impact on the physiological fluid or biological lubricant viscosity variations and, as a result, on the friction forces and friction coefficient. This paper describes the abovementioned impact and the process of friction forces and friction coefficients variations in biological friction nods.

Słowa kluczowe: smarowanie biohydrodynamiczne, ciecze fizjologiczne, lepkość, zwilżalność, stężenie jonów wodoru, siły tarcia, współczynniki tarcia.

Streszczenie

Z klasycznej teorii hydrodynamicznego smarowania wynika, że wzrost lepkości dynamicznej czynnika smarującego powoduje wzrost ciśnienia hydrodynamicznego, a także wzrost sił tarcia i zużycia. W przypadku dużych wartości ciśnienia widoczny jest jego wpływ na wartość współczynnika tarcia. Intensywny rozwój mikro-i nanotribologii przyczynił się do powstania wielu hipotez odnośnie do wzrostu i malenia współczynnika tarcia wraz ze wzrostem lepkości czynnika smarującego. Badania eksperymentalne dowiodły, że nawet w przypadku malenia współczynnika tarcia ze wzrostem lepkości oleju to spadki te są na ogół na tyle mniejsze od równoczesnych wzrostów ciśnienia, co w rezultacie doprowadza do wzrostu siły tarcia ze wzrostem lepkości.

W biologicznych węzłach tarcia rozmaity wpływ lepkości cieczy biologicznej na zmiany wartości sił tarcia oraz współczynnika tarcia uwidacznia się jeszcze bardziej. Wpływ ten jest powodowany dużym udziałem sił adhezji i kohezji pomiędzy cząsteczkami cieczy biologicznej opływającymi macierz komórkową dwuwarstwych fosfolipidów zalegających na chrząstce stawowej o zmiennej zwilżalności We i zmiennym stężeniu jonów wodorowych (pH). Zarówno We, jak i pH mają duży wpływ na zmiany lepkości cieczy fizjologicznej w szczególności cieczy synowialnej, które z kolei zmieniają wartości sił tarcia i współczynnik tarcia. Niniejsza praca opisuje i ilustruje mechanizm przedstawionych zmian i wpływów dla biologicznych węzłów tarcia.

[*] Technical University of Koszalin, Institute of Technology and Education, ul. Śniadeckich 2, 75-453 Koszalin, Poland, tel.+48 94 3478344, e-mail: krzysztof.wierzcholski@wp.pl.

[**] Gdynia Maritime University; Morska 81-87, 81-225 Gdynia; tel.+48585586348; e-mail: miszczak@wm.am.gdynia.pl.

INTRODUCTION

The topic of the presented paper concerns new principles of an impact of the real human joint living surfaces lubrication with phospholipids bilayer, wettability facilities, power hydrogen ion concentration on the physiologic fluid viscosity, surfaces energy and, finally, on the friction forces and friction coefficient.

The impact of adhesion and cohesion forces on pressure distribution and carrying capacity forces, and friction forces occurring during the lubrication of hydrodynamic, cylindrical, parabolic sidle microbearings where the journal diameter attains the value of about 10 millimeters and the micro-bearing gap height has values of up to one micrometre [**L. 1–6**] has been recently presented. Increments of pressure values in the biological and microbearing gap are presented in **Fig. 1**.

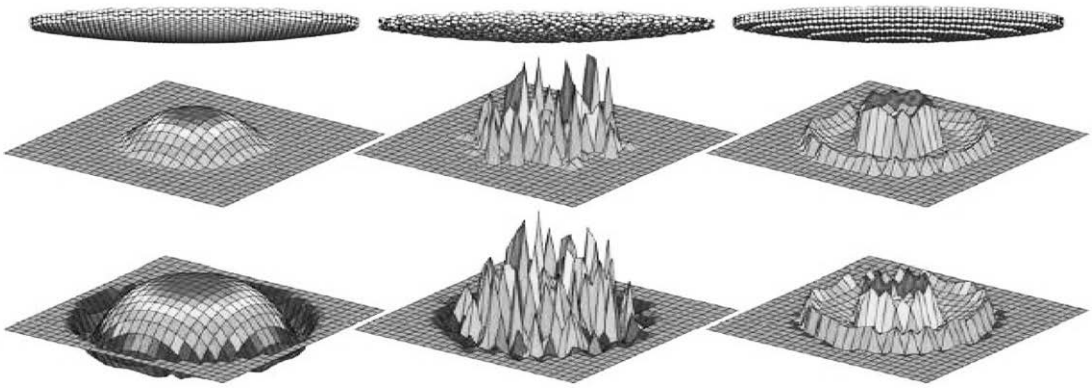

Fig. 1. Hydrodynamic pressure in biological and micro-gaps between cooperating surfaces, where the upper row shows solid surfaces, the middle row shows pressure without adhesion and the lower row illustrates pressure where adhesion forces are taken into account

Rys. 1. Ciśnienie hydrodynamiczne w mikroszczelinach pomiędzy współpracującymi powierzchniami bio- i mikrołożysk, przy czym pierwszy rząd od góry to powierzchnie ciała stałego, drugi rząd rysunków od góry pokazuje wartości ciśnienia bez uwzględnienia adhezji, trzeci rząd od góry to ciśnienie z uwzględnieniem adhezji

The author and his research team investigated the micro and nano-grooves situated in circumferential and longitudinal directions on the curvilinear journal surfaces. The grooves' shape and their location had an impact on the dynamic performances in the HDD micro-bearing, and adhesion had an impact on the pressure distribution and friction forces presented in **Figs. 2–4** [**L. 7–11**].

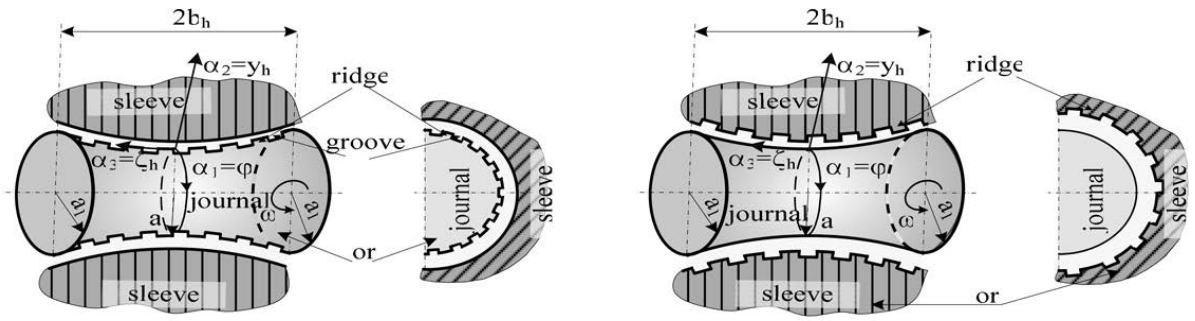

Fig. 2. View of hyperbolic journal or sleeve surfaces with ridges and grooves

Rys. 2. Rowki oraz żeberka na powierzchni hiperbolicznej czopa lub panewki w mikrołożysku

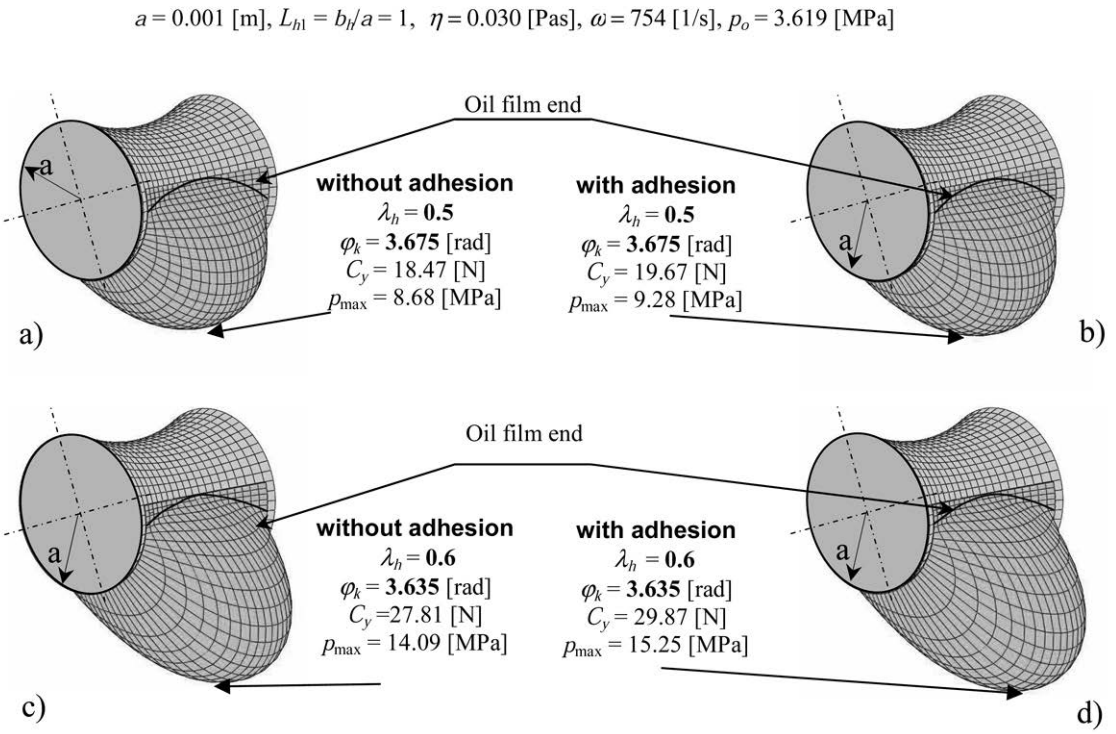

Fig. 3. Pressure distribution in hyperbolic micro-bearings caused by rotation in circumferential direction a, b) without the impact of adhesion forces on the oil viscosity, c, d) with viscosity changes caused by adhesion

Rys. 3. Rozkłady ciśnienia hydrodynamicznego w hiperbolicznym mikrołożysku: a, b) bez uwzględnienia sił adhezyjnych na lepkość czynnika smarującego, c, d) z uwzględnieniem sił adhezji na lepkość czynnika smarującego

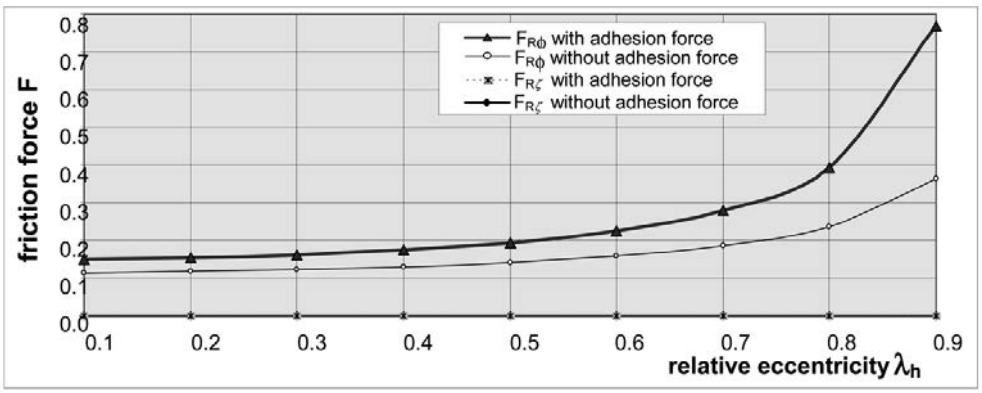

Fig. 4. Friction force components $F_{R\phi}$, $F_{R\zeta}$ with and without adhesion force impact

Rys. 4. Składowe sił tarcia w mikrołożysku z uwzględnieniem oraz z pominięciem sił adhezji

Figure 2 shows the groove and ridge geometry located on the hyperbolic surface. It can be observed that the grooves on the hyperbolic journal surfaces can be situated in the circumferential or longitudinal directions [**L. 2**]. The groove location affects the dynamic performance of the HDD spindle system. The hyperbolic micro-bearing lubrication is characterized by dynamic viscosity changes in the thin gap-height direction.

Figures 3a and **3c** show hydrodynamic pressure distribution inside a hyperbolic micro-bearing gap lubricated with a classical Newtonian lubricant for constant dynamic viscosity in the gap height direction without changes caused by adhesion and cohesion. **Figures 3b** and **3d** show hydrodynamic pressure distribution inside a hyperbolic micro-bearing gap lubricated with a classical Newtonian lubricant for variable dynamic viscosity in the gap height direction

where dynamic viscosity η is restricted between one and two values of viscosity caused by adhesion forces η_A (i.e. $\eta_A < \eta < 2\eta_A$). In this case, hydrodynamic pressure increases.

Figure 4 shows that the dynamic viscosity η increments in interval $\eta_A < \eta < 2\eta_A$ lead to the friction forces increases in the circumferential direction for a microbearing with a hyperbolic journal. For eccentricities 0.1 and 0.9, we obtain increases from 31% to 210%, respectively, in comparison to the friction values without the impact of adhesion. Friction forces in the longitudinal direction of the hyperbolic journal are negligible.

Now after our own calculations, we can observe the impact of the increments of the synovial fluid dynamic viscosity η on the changes of friction forces F_R and friction coefficient μ in the human hip joint if adhesion friction forces and the PL bilayer are not taken into account. Friction forces versus the dynamic viscosity of the synovial fluid and angular velocities of the hip bone head are presented in **Fig. 5**. It can be observed that, if the synovial fluid viscosity increases from 0.05 Pas to 0.45 Pas, and angular velocity increases, then the friction forces and friction coefficient increase as well.

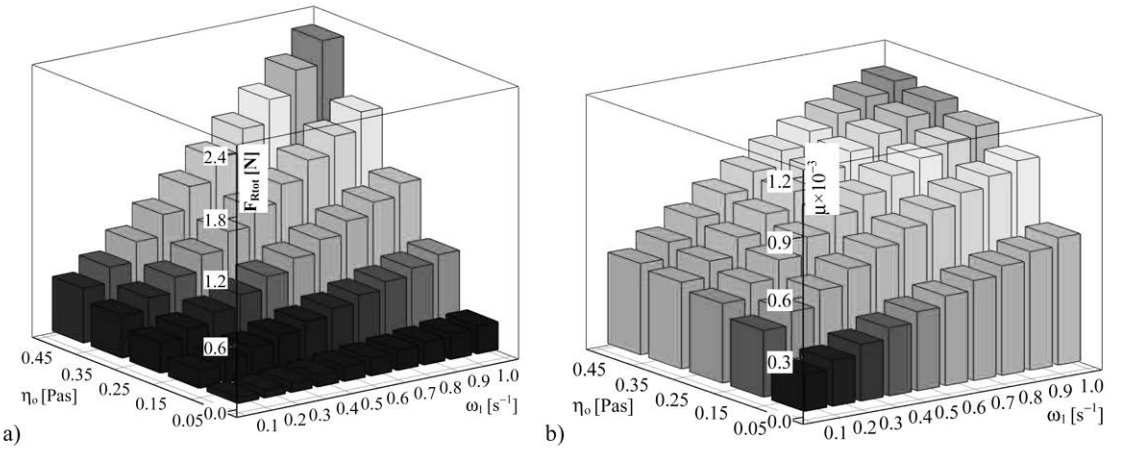

Fig. 5. Total values of friction forces a) and friction coefficient b) in human hip joint versus angular velocity of bone head and dynamic viscosity of the synovial fluid if adhesion friction forces and phospholipid bilayer are not taken into account

Rys. 5. Całkowite wartości sił tarcia a) i współczynnika tarcia b) w stawie biodrowym człowieka w zależności od prędkości kątowej sferycznej głowy kości udowej oraz lepkości dynamicznej cieczy synowialnej, gdzie siły tarcia od adhezji oraz warstwa fosfolipidów nie została uwzględniona

The measurements of friction forces in microbearings have been done by the author's research team at the University of Applied Science Giessen using Acoustic Emission [**L. 12–16**].

The experiments have shown that the generated AE depends on friction conditions within the hydrodynamic slide journal bearing gap. One can recognize the following dependences of the generated AE: (1) for the strength of the shear rate, namely, the higher the shear rate, the higher the generated AE, and (2) for the dynamic viscosity of the lubricant, namely, the higher the viscosity of the lubricant, the higher the generated AE.

So far, investigations and considerations have been taking into account only the impact of dynamic viscosity η increments in interval $\eta_A < \eta < 2\eta_A$ on friction forces and friction coefficients. Additionally, the impact of adhesion forces on oil velocity and friction force changes between cooperating biobearing surfaces coated with phospholipid bilayers have not been considered using analytical nor experimental methods. The present paper elaborates on the preliminary assumptions of the hydrodynamic theory of lubrication for a biobearing taking into account the significant impact of the PL bilayer on the lubricant or the synovial fluid viscosity and friction forces and friction coefficients. Moreover, the impact of significant adhesion forces on the friction coefficients for $\eta > 2\eta_A$ is considered.

For example, the surface of a cartilage human joint coated with phospholipid bi-layers or multi-layers, plays an important role in the surface active phospholipids (SAPL) lubrication, friction forces, friction coefficient, and wear during the human limb movement.

Research methods used in this paper include the following: the author's experience gained at German research institutes, experimental data obtained from measurements performed using the Bone Dias Apparatus in Germany, and practical results of measurements and information provided by patients.

The presence of phospholipid nano-particles in the synovial fluid during the human natural joint lubrication

provides for numerous positive effects, e.g., increments of viscosity and decrements of the friction coefficient values. Therefore, the results obtained in this paper may be applicable during the joint-endo-prosthesis or artificial joint design in new humanoid robots, where new soft materials with phospholipid additives are used instead of cartilage and the synovial fluid.

Variations of the synovial fluid dynamic viscosity and the friction coefficient and friction force values presented on the basis of tribology methods derived from boundary ultra-thin layer non-Newtonian lubrication assumptions are implemented by conjugated hydro- hyper-elastic fields, using new mathematical and numerical calculation methods and comparisons using experimental data.

BIO-BOUNDARY LAYER WITH ADHESION FORCES

The mechanism of lubrication for the various geometrical cartilage shapes coated with a phospholipids membrane requires us to account for, in the presented considerations, the form of elaboration in the curvilinear coordinates. The synovial fluid has non-Newtonian properties, due to the presence of the phospholipids and collagen particles. The very thin lipid bilayer is resting on the cartilage superficial layer surface and establishes a thin polar membrane of lipid molecules. These membranes are flat sheets that form a continuous barrier around the cells. The lipid bilayer is a barrier that keeps ions and proteins where they are needed and prevents them from diffusing into areas where they should not be. Negatively charged ions with sodium counter captions strongly hydrated in the synovial fluid are lying on the superficial bilayer. The PL-bilayer lining the hydrophilic negatively charged cartilage surfaces in natural joints implemented with classical friction forces FR and adhesion friction forces FA are presented in **Fig. 6**.

In **Fig. 6**, we have the following notations: 1 – PL – bilayer, 2 – hydrated $–PO_4^-$ group, 2* – hydrated sodium ions, 3 – synovial fluid, 4 – collagen and cartilage region, 5 – liposome occurring in synovial fluid, and W – Load, P_N – hydrodynamic pressure force, R – repulsion force,

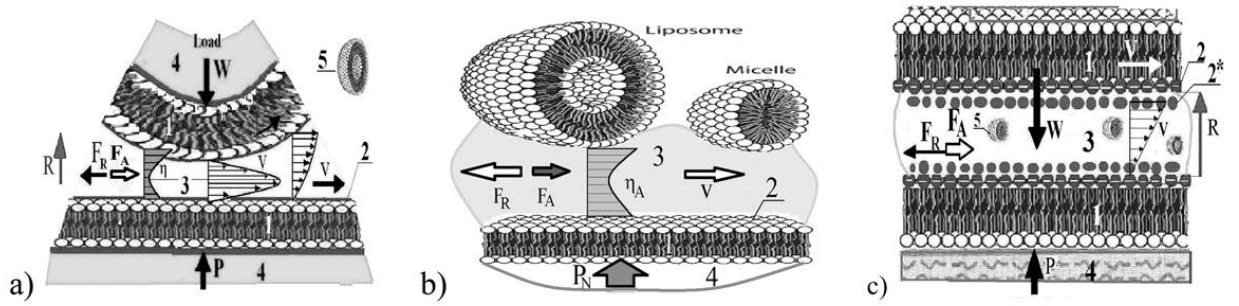

Fig. 6. Joint gap lubrication limited by the phospholipid (PL) bilayer of various surface shapes between: a) right lineas and spherical, b) right linear and liposome c) two right-linear for flat motion

Rys. 6. Szczelina stawu ograniczona dwuwarstwą fosfolipdów o różnym kształcie pomiędzy powierzchniami: a) płaską i sferyczną, b) płaską i sferyczną liposomu, c) dwoma prostoliniowymi

V – velocity of the upper surface, F_R – friction force, F_A – adhesion friction force, η – viscosity distribution of synovial fluid. **Fig. 6** illustrates forces acting in the numerous human joint gaps of various shapes. These gaps are limited by the upper and lower phospholipid membrane (PL-bilayer) and filled with the synovial fluid. Here we can observe the repulsive force R caused by the negatively charged phospholipids membrane, especially of the $(-PO_4^-)$ groups, with sodium counter-cations, which are strongly hydrated in the presence of the synovial fluid. Such charged surfaces can be observed on both external PL bilayer surfaces in contact with the synovial fluid. There is the load carrying capacity force denoted by the letter P_N and friction force F_R caused by the hydrodynamic pressure obtained from the rotation of the cartilage surface on the bonehead or by squeezing during the lubrication process. Friction force F_A caused by the adhesion force and friction force F_R has, in general, the same lines and opposite senses. The lines of forces R and P_N are the same. The load force W of the presented human joint has, in PN, the reverse sense and the same line as the forces P_N and R. Hence, the carrying capacity force has the repulsive force R which counteracts and opposes the load force W.

Transverse sections of curvilinear joint gaps surfaces presented in **Figs. 6b**, **c** have, among others, spherical, cylindrical, parabolic, and hyperbolic shapes, depending on the type of normal and pathological human joint and depending on the cartilage surface irregularities and roughness. Irregularities of the cartilage surfaces have values from 1 to 5 micrometres. The Young modulus of elasticity of the considered cartilage has values from 12 to 50 MPa. The compressive and bending strength of a sound (20–30 years old) human bone attains the value

of 20 MPa. The Young modulus of elasticity of a sound (20–30 years old) human bone attains the value of value 20 GPa.

GOVERNING EQUATIONS

To determine the impact of the synovial fluid viscosity and adhesion forces on the friction effects, a semi analytical method of the solution of the asymmetrical, non-stationary, laminar, non-Newtonian synovial fluid flow lubrication between two rotational squeezing and curvilinear orthogonal movable cartilage surfaces coated with the PL bi- layer is presented. The inertia forces of the synovial fluid are negligible, because the speed of liquid particles in a human gap joint during the limb motion attains values usually not exceeding 2 m/s. To include or exclude the direct impact of an electric intensity field generated on the PL membrane surface on the tribology properties and to indicate the indirect impact of electric intensity on the synovial fluid viscosity changes, we neglect the body forces except for the Lorentz forces. Based on the author's own studies and scientific literature data, it can be stated that temperature variations in an interval between 34°C and 43°C occurring usually in the human body affect the tribology parameters during the SAPL lubrication, if and only if, we consider the temperature impact on the collagen fibre consistency and pH ion concentration in the synovial fluid and indirectly on the liquid viscosity effects. Thus, the mathematical 3D model of SAPL hydrodynamic joint lubrication includes the conservation of energy equation and the Young-Kelvin-Laplace equation describing the interfacial energy in the cartilage superficial layer. The velocity of bio-fluids and accelerations in human joints are relatively small, thus are neglected here, together with local derivatives as convection and convection energy terms, pressure dissipation energy terms. Heat Joule terms are also considered. The 3D synovial fluid flow between the two abovementioned solid cartilage surfaces in the electromagnetic field will be described in a vector form using the three equations of the equilibrium of momentum, with a fluid continuity Equation (1), and in scalar form using the conservation of energy Equation (2), and the Young-Kelvin-Laplace Equation (3). The mentioned equations are as follows:

$$\mathrm{Div}\,\mathbf{S} + \rho_e \mathbf{E} = 0, \quad \frac{\partial \rho}{\partial t} + \mathrm{div}(\rho \mathbf{v}) = 0 \tag{1}$$

$$\mathrm{div}(\kappa\,\mathrm{grad}\,T) + \varphi_F = J^2/\sigma \tag{2}$$

$$\gamma = \gamma_{max} + 2sR_gT\ln\left(\sqrt{\frac{K_a}{K_b}} + 1\right) - sR_gT\ln\left[\left(\frac{K_a}{a_H^+} + 1\right)\left(\frac{a_H^+}{K_b} + 1\right)\right] \tag{3}$$

where

- S − stress tensor in the synovial fluid [Pa],
- E – electrostatic intensity vector in PL [V/m],
- J − electric current density in [A/m_2],
- T − synovial fluid temperature [K],
- ρ_ε − electric space charge in the synovial fluid [C/m^3 = As/m^3],
- κ − thermal conductivity coefficient for the synovial fluid [W/mK],
- φ_F – dissipation of energy [W/m^3],
- R_g − gas constant (8.3144598 J/(mol·K)),
- $s = (NA \cdot A)^{-1}$ − concentration of PL particles [mol/m^2],
- γ − interfacial energy [J/m^2 = N/m],
- γ_{max} − is the maximum interfacial energy of the lipid membrane,
- K_a − acid equilibrium constant (denotes how much energy is needed to stretch the bi-layer) [J],
- K_b − base equilibrium constant (denotes how much energy is needed to bend or flex the bi-layer) [J],
- a_H − protons energy activity [J],
- A − cartilage surface coated by the PL molecules [m^2],
- $N_A = 6.024 \cdot 1023$ − Avogadro number,
- ρ − synovial fluid density in [kg/m^3],
- σ − electrical conductivity of the PL bi-layer [S/m].

The synovial fluid flow in a human joint gap is strictly dependent upon the energetic statement of the hyper-elastic cartilage.

Because of the presence of the phospholipids bi-layers on the cartilage surface and the presence of liposomes, micelles, macromolecules, and lamellar aggregates in the synovial fluid, this liquid has non-Newtonian, especially, pseudo-plastic, properties. Constitutive equations of the Reiner-Rivlin type for the abovementioned synovial fluid well describe the non-linear dependences between stresses and shear rates; whereas, the apparent viscosity and consistency coefficient depends mainly on the shear rate of the synovial fluid flow, the electrostatic field occurring on the PL-bi-layers, cartilage wettability, power hydrogen ion concentration in the synovial fluid, collagen fibre concentration in the synovial fluid, and to a lesser extent, the temperature. For the synovial fluid, the relationship between stress tensor S and displacement velocity tensor $2Td = \Theta$, i.e. constitutive equations is applied in the following form [**L. 17**]:

$$\mathbf{S} = -p\boldsymbol{\delta} + \eta_p \boldsymbol{\Theta} \tag{4}$$

Unit tensor δ and strain tensor Θ have the following components: δ_{ij}, Θ_{ij} [s^{-1}]. We denote them as follows: δ_{ij} − Kronecker Delta, p − pressure [Pa]. For a non-Newtonian synovial fluid of the Reiner-Rivlin type, the constitutive dependences between apparent viscosity η_p [Pas] have the following form [**L. 17–19**]:

$$\eta_p(\alpha_1,\alpha_2,\alpha_3,t)=\eta_p(n,p_H,We,T,t,E,E_X)\equiv m(n,p_H,We,T,t,E,E_X)\left|\left(\frac{\partial v_1}{\partial\alpha_2}\right)^2+\left(\frac{\partial v_3}{\partial\alpha_2}\right)^2\right|^{\frac{n-1}{2}} \tag{5}$$

where

n − dimensionless flow index dependent on the PL concentration in the synovial fluid,

m = m(n, T, t, p_H, We) − fluid consistency coefficient in [Pas^n],

h_i − Lame coefficients,

We − cartilage wettability,

p_H − power hydrogen ion concentration,

t − time.

Relations between shear rate Θ_{ij} and the synovial fluid velocity components v_i [m/s] are as follows [**L. 17–19**]:

$$\Theta_{ij}=\frac{1}{2}\left[\frac{h_i}{h_j}\frac{\partial}{\partial\alpha_j}\left(\frac{v_i}{h_i}\right)+\frac{h_j}{h_i}\frac{\partial}{\partial\alpha_i}\left(\frac{v_j}{h_j}\right)+2\delta_{ij}\sum_{k=1}^{3}\frac{v_k}{h_i h_k}\frac{\partial h_i}{\partial\alpha_k}\right] \tag{6}$$

We denote as follows: We − wettability of cartilage in an interval from 30° for hydrophiling cartilage to 100° for hydrophobic cartilage, v_0 − characteristic value of linear velocity of the synovial fluid in a joint gap (average limb velocity) from 0.25 to 4.0 [m/s], δ_v − dimensionless coefficient introduced by the author in range ($2 < \delta_v < 6$) determining in the synovial fluid the variations of concentration of nano-meter long collagen fibres from $\delta_v = 2$ for cc = 1 000 000 mol/mm^3 to cc = 100 mol/mm^3 and less for $\delta_v = 6$, E − electric intensity charges, E_X − module or modules of elastic or hypoelastic cartilage. Curvilinear, orthogonal coordinates are as follows: α_1 − circumferential direction, α_2 − gap height direction, α_3 − longitudinal direction. Assuming the PL-bilayer in human joint lubrication we take into account the following typical experimental data: power acid equilibrium constant pK_a = 2.58, power base equilibrium constant pK_b = 5.98, maximum interfacial energy of the lipid membrane γ_{max} = 4.0 mJ/m^2, average limb velocity v_0 =1.0 m/s, collagen concentration fibres in the synovial fluid δ_v = 6 so that $\delta_v v_0$ = 6 m/s, lubricated cartilage surface A = 0.00025 m^2, synovial fluid density ρ = 1010 kg/m^3.

ADHESION IMPACT WITH A PL-BILAYER ON THE FRICTION FORCES EFFECTS

The time t dependent components of friction forces in curvilinear α_1 and α_3 directions occurring in human joint gaps with a PL-bilayer have the following forms:

$$F_{R1}(t)=\iint_{\Omega}\left(\eta\frac{\partial v_1}{\partial\alpha_2}\right)_{\alpha_2=\varepsilon_T}h_1h_3d\alpha_1d\alpha_3,\quad F_{R3}(t)=\iint_{\Omega}\left(\eta\frac{\partial v_3}{\partial\alpha_2}\right)_{\alpha_2=\varepsilon_T}h_1h_3d\alpha_1d\alpha_3 \tag{7}$$

where

$0\le\alpha_1\le2\pi\theta_1$, $0\le\theta_1\le1$, $b_m\le\alpha_3\le b_s$, $0\le\alpha_2\le\varepsilon_T$, $\varepsilon_T=\varepsilon_T(\alpha_1,\alpha_3)$, $\eta(\alpha_1,\alpha_2,\alpha_3)$, $\Omega(\alpha_1,\alpha_3)$ − lubrication surface,

$\varepsilon_T(\alpha_1,\alpha_3)$ − gap height, $\eta(\alpha_1,\alpha_2,\alpha_3)=\eta(n,p_H,We,T,t,E,E_x)$ – fluid dynamic viscosity. By solving equations (1)–(5) we obtain pressure p and v_1, v_3 – the synovial fluid velocity components in α_1, α_3 directions, respectively. The human joint load carrying capacity P_N [N] in curvilinear coordinates of two cooperating cartilage surfaces can be calculated from the following formula:

$$P_N^{(\alpha)}=\sqrt{\left[\int_0^{+2b_d}\left(\int_0^{\phi_k}p(\alpha_1,\alpha_3)h_1(\sin\alpha_1)d\alpha_1\right)d\alpha_3\right]^2+\left[\int_0^{+2b_d}\left(\int_0^{\phi_k}p(\alpha_1,\alpha_3)h_1(\cos\alpha_1)d\alpha_1\right)d\alpha_3\right]^2} \tag{8}$$

where symbol ϕ_k denotes the end coordinate of the film in the circumferential α_1 direction of the bone head and we have: $0\le\alpha_1\le\phi k<2\pi$, $0\le\alpha_3\le2b_d$, $\varepsilon_T=\varepsilon_T(\alpha_1,\alpha_3)$, 2 b_d-bone head length in the longitudinal direction.

Using the Coulomb Law Friction, taking into account friction caused adhesion forces F_A [N], the dimensionless friction forces coefficients in curvilinear coordinates have the following form:

$$\mu_\alpha = \frac{\left|e_1 F_{R1} + e_3 F_{R3}\right| - F_A}{P_N^{(\alpha)}} \tag{9}$$

where e_1, e_3 are the unit vectors in the circumferential α_1 and longitudinal α_3 directions.

Among recently published papers [**L. 19–21**] concerning human joint lubrication, we can find numerous papers presenting experimental data referring to the impact of PL concentration, cartilage wettability, and power hydrogen concentration pH on the friction coefficient [**L. 20**]. The researches indicated the decrements of friction coefficients from 1.00 to 0.01, if PL concentration, δv, increases in arbitrary units from 1 to 4. A trial of mathematical methods of analysing the impact of PL concentration on the joint friction coefficient at a molecular level was undertaken by A. Gadomski et.al. [**L. 21**], where, after solving molecular energy equations, dependences were obtained determining slow increases of the friction coefficient in time and on the ground of the flexural dissipation law, which enable us to show the dependence of viscosity decreases in time for constant temperature. Finally, it may be concluded that viscosity is inversely proportional to the friction coefficient.

From the classical theory of lubrication, it may be concluded that increments of dynamic viscosity of the lubricant result in the increments of load carrying capacity and finally increments of friction forces. Z. Pawlak and A. Bojan [**L. 20–21**], in their own researches, stipulated that the local high value of dynamic viscosity in the synovial fluid cannot be in contradiction with the low value of the friction coefficient. A confirmation of this statement had been motivated on the grounds of molecular chemise [**L. 19–21**]. The abovementioned results were motivated by the author of this paper on the grounds of the hydrodynamic theory of lubrication (4)–(5) and his own experiences. For a low Reynolds number $0 < Re < 1$ occurring in human joints during the human limb motion and neglecting the adhesion friction forces $F_A = 0$, then accordingly, of Amontonson law and presented in this paper the hydrodynamic theory (4)–(5), we obtain the following relations between friction force F_R [N], load capacity P_N [N], and dimensionless friction coefficient μ:

$$F_R = \frac{\eta U S}{\varepsilon_T}, \quad P_N = \frac{R_\rho^2 \cdot \eta^2}{\varepsilon_T^2 \cdot \rho} = p_0 R_\rho^2, \quad p_0 = \frac{\eta^2}{\varepsilon_T^2 \cdot \rho} = \frac{U\eta}{Re \cdot \varepsilon_T}$$
$$F_R = \mu P_N, \quad \mu = \frac{US\rho\varepsilon_T}{\eta R_\rho^2} = Re \cdot \left(\frac{S}{R_\rho^2}\right), \quad Re \equiv \frac{U\rho\varepsilon_T}{\eta}, \tag{10}$$

where η − dynamic viscosity of biological liquid [Pas], U − linear velocity of the bio-surface [m/s], S − region of cooperating biosurfaces [m^2], ε_T − average value of total gap height in [m] in the range of cooperating surfaces, p_0 − characteristic value of pressure in [Pa], ρ − density of the biological fluid in range from 700 to 1150 kg/m^3, R_ρ − curvature radius of cooperating joint surfaces in [m].

From the governing Equations (4)–(5) and Equation (10) it follows that increments of the synovial fluid dynamic viscosity result in increments of hydrodynamic pressure p_0 and then increases in friction forces F_R and decreases in the friction coefficient μ, because increments of the carrying capacity PN are larger than decrements of the friction coefficient μ. Finally, from Equation (10), it follows that increments of the synovial fluid dynamic viscosity result in decrements of friction coefficient because of decreases in the value of the Reynold's number $Re = U\varepsilon_T\rho/\eta$.

Therefore, considering the values from (8)–(9) denoting adhesion friction forces by F_A, thus by virtue of dependences (10), we obtain the total friction coefficient μ and load capacity P_N in following form:

$$\mu = Re \cdot \frac{S}{R_\rho^2} - \frac{F_A}{P_N}, \quad P_N = \frac{R_\rho^2 \cdot \eta^2}{\varepsilon_T^2 \cdot \rho} = \frac{1}{Re} \cdot \frac{R_\rho^2}{S} \cdot \frac{US\eta}{\varepsilon_T} \tag{11}$$

The quotient F_A/P_N denotes the friction coefficient decrements caused by the adhesion forces. Hence, the total friction coefficient has the form:

$$\mu = Re \cdot \frac{S}{R_\rho^2} - \frac{F_A}{P_N} = Re \cdot \frac{S}{R_\rho^2} - \frac{F_A Re S \varepsilon_T}{R_\rho^2 US\eta} = Re \cdot \frac{S}{R_\rho^2}\left(1 - \frac{F_A}{\frac{US\eta}{\varepsilon_T}}\right) \tag{12}$$

Determining the adhesion friction forces F_A [N] by the characteristic dynamic viscosity η_A [Pas] obtained from adhesion forces and denoting and defining the characteristic value of dynamic viscosity of the biological liquid η_0 [Pas] without the adhesion impact in the following form:

$$F_A \equiv \frac{US\eta_A}{\varepsilon_T}, \quad \eta = \eta_0\eta_1, \quad \eta_0 \equiv \frac{US\rho\varepsilon_T}{R_\rho^2} \geq 10^{-4}\,\text{Pas} \tag{13}$$

Thus, changing the assumed viscosity value η_0 from (13) into the reverse value of dimensionless viscosity $1/\eta_1$ and taking into account Reynolds number definition, we obtain th following:

$$\frac{1}{\eta_1} = \frac{\eta_0}{\eta_0\eta_1} = \frac{\eta_0}{\eta} = \frac{1}{\eta}\cdot\left(\frac{US\rho\varepsilon_T}{R_\rho^2}\right) = \left(\frac{U\rho\varepsilon_T}{\eta}\right)\frac{S}{R_\rho^2} = \text{Re}\cdot\frac{S}{R_\rho^2} \tag{14}$$

Substituting adhesion friction forces F_A [N] defined in (13) and the result of calculation (14) into the result of Expression (12) produces the total friction coefficient in the following form:

$$\mu(\eta_1) = \frac{1}{\eta_1}\left(1 - a_1\frac{1}{\eta_1}\right), \quad a_1 \equiv \frac{\eta_A}{\eta_0}, \quad \eta_1 > a_1 \tag{15}$$

For an ultra-thin biological layer, the dimensionless parameter a_1 attains values (> 100) and describes the ratio of the characteristic lubricant dynamic viscosity caused by the adhesion forces η_A to the characteristic lubricant viscosity η_0 in the case when adhesion forces are neglected η_0.

From Formula (15), it follows that dimensionless friction coefficient μ increases if dimensionless lubricant dynamic viscosity η_1 increases in dimensionless interval $a_1 < \eta_1 < 2a_1$ and friction coefficient μ decreases in dimensionless interval $\eta_1 > 2a_1$. This result is presented in **Fig. 7**.

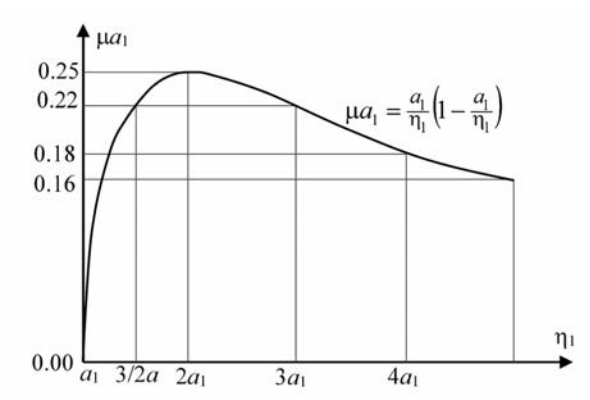

Fig. 7. Friction coefficient versus viscosity in biological adhesive conditions

Rys. 7. Wpływ lepkości na współczynnik tarcia w warunkach biologicznej adhezji

RESULTS FROM NUMERICAL CALCULATIONS

The friction coefficient variation depends on the various kinds of lubrication and the synovial fluid various features, such as power hydrogen concentration pH, wettability We, shear rate Θ, and collagen fibre concentration, obtained using analytical calculations of Equations (1)–(8) presented in **Tables 1** and **2** with and without adhesion forces.

1. The changes of wettability, We, from hydrophobic to hydrophilic, decrease the synovial fluid viscosity, see **Fig. A2** [**L. 22**], hence, by virtue of (10) without adhesion friction forces ($F_A = 0$), the second row in **Tab. 1** indicates increases in the friction coefficient and decreases in load PN and decreases in friction force F_R.
2. pH increases 2.0 < pH <3.7, which increases the synovial fluid viscosity, **Fig. A1**, [**L. 22**]; hence, by virtue of (10) without adhesion forces ($F_A = 0$), the third row (point a) in **Tab. 1** indicates decreases in friction coefficient μ and increases load P_N and increases friction force F_R.
3. pH increases 3.7 < pH < 12, which decreases the synovial fluid viscosity, **Fig. A1** [**L. 22**]; hence, by virtue of (10) without adhesion forces ($F_A = 0$), the third row (point b) in **Tab. 1** indicates the increases in friction coefficient μ and decreases load P_N and decreases friction force F_R.
4. The shear rate values Θ in the synovial fluid flow decrease the synovial fluid viscosity [**L. 22**]; hence, by virtue of (10) without adhesion forces ($F_A = 0$), the forth row in **Tab. 1** indicates the increases in friction coefficient μ and decreases load P_N and decreases friction force F_R.
5. The synovial fluid dynamic viscosity η in interval $\eta_A < \eta < 2\eta_A$ increases the friction coefficient μ for $F_A > 0$ by virtue of equation (15) and, additionally, the changes of wettability We, from hydrophobic to hydrophilic, decreases the synovial fluid viscosity, see **Fig. A2** [**L. 22**], hence, by virtue of (10), increases

the friction coefficient μ. The second row (point a) in **Tab. 2** indicates the friction coefficient μ increases.

6. The synovial fluid dynamic viscosity η in interval $\eta > 2\eta_A$ decreases the friction coefficient μ for $F_A > 0$ by virtue of Equation (15). Independently, the changes of wettability, We, from hydrophobic to hydrophilic, decrease the synovial fluid viscosity, see **Fig. A2** [**L. 22**], hence, by virtue of (10), increases the friction coefficient. But these increases can be often lower than decreases in the friction coefficient for $\eta > 2\eta_A$. Finally, the second row 2 (point b) in **Tab. 2** generally indicates the unidentified friction coefficient μ changes decreases.
7. The synovial fluid dynamic viscosity η in interval $\eta > 2\eta_A$ decreases the friction coefficient μ for $F_A > 0$ by virtue of equation (15) and additionally the changes of pH in interval $2.0 < pH < 3.7$, increases the synovial fluid viscosity, see **Fig. A1** [**L. 22**], hence, by virtue of (10), decreases the friction coefficient. Finally, the third row (point Ib) in **Tab. 2** indicates the friction coefficient decreases.
8. The synovial fluid dynamic viscosity η in interval $\eta_A < \eta < 2\eta_A$ increases the friction coefficient μ for $F_A > 0$ by virtue of equation (15) and additionally the changes of pH in interval $3.7 < pH < 12$ decreases the synovial fluid viscosity, see **Fig. A1** [**L. 22**], hence, by virtue of (10), increases the friction coefficient. Finally, the third row (point IIa) in **Tab. 2** indicates the friction coefficient μ increases.

Table 1. The numerous variations in the synovial fluid friction coefficient function without adhesion forces ($F_A = 0$) during the non-Newtonian lubrication for $0 < Re < 1$ of two co-operating non-homogeneous, hyper-elastic cartilage surfaces coated with a PL-bilayer in human joints, using characteristic viscosity value: $\eta_0 = US\rho\varepsilon_T/(R_\rho)^2 = 0.0006$ Pas, for: U − linear velocity of the bio-surface [m/s], S − region of cooperating biosurfaces [m^2], ε_T − average value of the total gap height, ρ − density of the biological fluid from 700 to 1150 kg/m^3, R_ρ − curvature radius of cooperating joint surfaces in m, whereas $Re = U\rho\varepsilon_T/\eta$

Tabela 1. Zmiany wartości współczynnika tarcia bez uwzględnienia sił adhezji ($F_A = 0$) podczas nienewtonowskiego smarowania dla $0 < Re < 1$ dwóch współpracujących niejednorodnych hiper-sprężystych powierzchni chrząstek pokrytych warstewką fosfolipidów w stawach człowieka przyjmując charakterystyczną lepkość cieczy $\eta_0 = US\rho\varepsilon_T/(R_\rho)^2 = 0{,}006$ Pas, gdzie: U − liniowa prędkość powierzchni stawu [m/s], S − obszar współpracujących powierzchni stawu [m^2], ε_T − średnia wysokość szczeliny stawu, ρ − gęstość cieczy synowialnej 700 to 1150 kg/m^3, R_ρ − promień krzywizny powierzchni stawowych m, gdzie $Re = U\rho\varepsilon_T/\eta$

No	Non –Newtonian Synovial fluid in a natural sound human joint for η_0=0.006Pas, F_A=0, 0<Re<1		Features of a cartilage human sound joint assigned to the successive calculated changes of friction coefficients	Type of lubrication assigned to changes of successive friction coefficients
	The friction coefficients μ with corresponding anticipated changes of other parameters	The obtained values of intervals for friction coefficients variations depending on other data		
1	Friction coefficient μ increments with temperature increases	0.020 <μ< 0.200, if: 35°C <T<44°C, for We=40°, pH=6, $v\delta_v$=6m/s,c_c=5·10^{5}mol/mm^3	Isotropic, homogeneous, Elastic, constant Young modulus E from 12 to 50 MPa	Rotation, squeezing
2	Friction coefficient μ increments along wettability from hydrophobic (70°) to hydrophilic (50°), for η_0=0.006Pas,	0.015 <μ< 0.020, if:70°>We>50°, for: pH=6, T=37°C, $v\delta_v$=6m/s,c_c=5·10^{5}mol/mm^3	Isotropic, homogeneous, Elastic, constant Young modulus E from 12 to 50 MPa	Rotation, squeezing
3	Friction coefficient μ: a) decrements, b) increments, with pH index increases,	a): 0.200 >μ> 0.011 if: 2.0<pH<3.7, b): 0.011 <μ< 0.30 if: 3.7<pH<12, for a,b: We=40°, T=37°C, $v\delta_v$=6m/s, c_c=5·10^{5}mol/mm^3	Isotropic, homogeneous, Elastic, constant Young modulus E from 12 to 50 MPa	Rotation, squeezing
4	Friction coefficient μ increments for shear rate values Θ increments for the synovial fluid and other pseudo-plastic lubricants.	0.020 <μ< 0.200 , if: 5 s^{-1}<Θ<10^4 s^{-1}, for : We=40°,T=37°C, $v\delta_v$=6m/s,c_c=5·10^{5}mol/mm^3 2<pH<12.0,	Isotropic, homogeneous, Elastic, constant Young modulus E from 12 to 50 MPa	Rotation, squeezing
5	Friction coefficient μ decrements with increases in phospholipids and collagen fibres molecules concentration for $v\delta_v$=6m/s,	0.200 >μ>0.015, if:10 <c_c<10^{6}mol/ mm^3, (8>δ_v>2), for: 3.7<pH<12, 70°>We>50°,	Isotropic, homogeneous, Elastic, constant Young modulus E from 12 to 50 MPa	Rotation, squeezing
6	Friction coefficient μ increments of non-treated synovial fluid during the time t in years after statistical observation, and calculations	$\mu(t=t_0) < \mu < \mu(t=t_1)$, if: $(t_0=0)<t<(t_1=10$ years)	Anisotropic, non-homogeneous, Hyper-elastic, 21 various Hyper-elastic modules E from 12 to 60 MPa	Rotation, squeezing

Table 2. The numerous interval values of multivariable fluid friction coefficient taking into account adhesion forces ($F_A > 0$) during the non-Newtonian lubrication for $0 < Re < 1$, in view of mutual connections of features of two co-operating non-homogeneous, hyper-elastic cartilage surfaces coated with PL-bilayer in human joints, using the ratio $a_1 = \eta_A/\eta_0 > 100$ of characteristic viscosity value with and without adhesion: $\eta_0 = US\rho\varepsilon_T/(R_\rho)^2 = 0.0006$ Pas, for: U − linear velocity of bio-surface [m/s], S − region of cooperating biosurfaces [m^2], T − average value of total ultra thin gap height, ρ − density of biological fluid from 700 to 1150 kg/m^3, R_ρ − curvature radius of cooperating joint surfaces in m, whereas $Re = U\rho\varepsilon_T/\eta$

Tabela 2. Zmiany wartości współczynnika tarcia z uwzględnieniem sił adhezji ($F_A > 0$) podczas nienewtonowskiego smarowania dla $0 < Re < 1$ dwóch współpracujących niejednorodnych hipersprężystych powierzchni chrząstek pokrytych warstewką fosfolipidów w stawach człowieka przyjmując $a_1 = \eta_A / \eta_0 > 100$ dla charakterystycznej lepkości cieczy $\eta_0 = US\rho\varepsilon_T/(R_\rho)^2 = 0.0006$ Pas, gdzie: U − liniowa prędkość powierzchni stawu [m/s], S − obszar współpracujących powierzchni stawu [m^2], ε_T − średnia wysokość szczeliny stawu, ρ − gęstość cieczy synowialnej 700 to 1150 kg/m^3, R_ρ − promień krzywizny powierzchni stawowych m, gdzie $Re = U\rho\varepsilon_T/\eta$

No	Non –Newtonian Synovial fluid in a natural sound human joint for $a_1>0$, $\eta_0=0.006$Pas, $F_A>0$, $0<Re<1$		Features of a cartilage human sound joint assigned to the successive calculated changes of friction coefficients	Type of lubrication assigned to changes of successive friction coefficients
	The friction coefficients μ with corresponding anticipated changes of other parameters	The obtained values of intervals for friction coefficients μ variations depending on other data		
1	Friction coefficient μ changes for: a) $a_1<\eta_1<2a_1$, b) if $\eta_1>2a_1$ with temperature increases	a) μ increases, b) μ decreases if: 35°C <T<44°C, for We=40°, pH=6, $v\delta_v$=6m/s, $c_c=5\cdot10^5$mol/mm^3	Isotropic, homogeneous, Elastic, constant Young modulus E from 12 to 50 MPa	Rotation, squeezing
2	Friction coefficient μ changes for: a) $a_1<\eta_1<2a_1$, b) if $\eta_1>2a_1$,along wettability from hydrophobic (70°) to hydrophilic (50°), for η_0=0.006Pas,	a) μ increases, b) μ not identified changes if:70°>We>50°, for: pH=6, T=37°C, $v\delta_v$=6m/s, $c_c=5\cdot10^5$mol/mm^3	Isotropic, homogeneous, Elastic, constant Young modulus E from 12 to 50 MPa	Rotation, squeezing
3	Friction coefficient μ changes for: a) $a_1<\eta_1<2a_1$, b) if $\eta_1>2a_1$, with pH index increases,	I: a) μ-not identified changes, b) μ-decreases if: 2.0<pH<3.7, II: a) μ increases, b) not identified changes if: 3.7<pH<12, for a, b: We=40°,T=37°C, $v\delta_v$=6m/s, $c_c=5\cdot10^5$mol/mm^3	Isotropic, homogeneous, Elastic, constant Young modulus E from 12 to 50 MPa	Rotation, squeezing
4	Friction coefficient μ changes for: a)$a_1<\eta_1<2a_1$, b) if $\eta_1>2a_1$, with shear rate values Θ increments for the synovial fluid and other pseudo-plastic lubricants,	a) μ increases, b) μ decreases, if: 5 $s^{-1}<\Theta<10^4$ s^{-1}, for : We=40°, T=37°C, $v\delta_v$=6m/s, $c_c=5\cdot10^5$mol/mm^3 2<pH<12.0,	Isotropic, homogeneous, Elastic, constant Young modulus E from 12 to 50 MPa	Rotation, squeezing
5	Friction coefficient μ changes for: a) $a_1<\eta_1<2a_1$, b) if $\eta_1>2a_1$,with increases in phospholipids and collagen fibres molecules concentration for $v\delta_v$=6m/s,	a) μ increases, b) μ decreases, if:10 <$c_c<10^6$mol/ mm^3, (8>δ_v>2), for: 3.7<pH<12, 70°>We>50°,	Isotropic, homogeneous, Elastic, constant Young modulus E from 12 to 50 MPa	Rotation, squeezing
6	Friction coefficient μ: a) increases if $a_1<\eta_1<2a_1$,b) decreases, if $\eta_1>2a_1$, of non-treated synovial fluid during the time t increases in years after statistical calculations observation,	a) $\mu(t=t_0) < \mu < \mu(t=t_1)$, b) $\mu(t=t_0) > \mu > \mu(t=t_1)$, if: $(t_0=0)<t<(t_1=10$ years)	Anisotropic, non-homogeneous Hyper-elastic, 21 various Hyper-elastic modules E from 12 to 60 MPa	Rotation, squeezing

APPENDIX

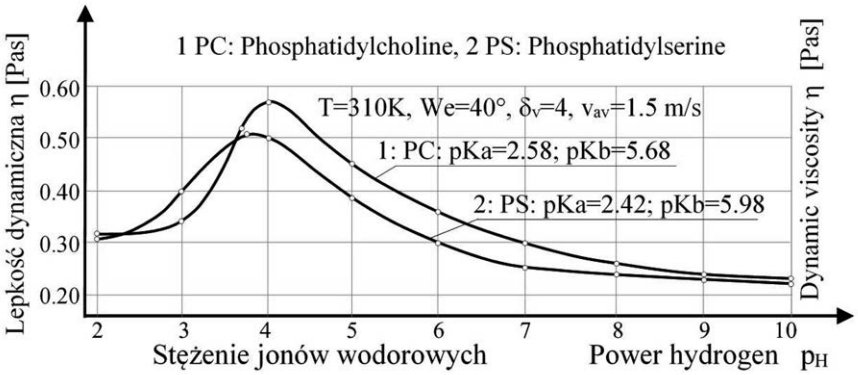

Fig. A1. Dynamic viscosity increments for 0 < pH < 4 and decrements for pH > 4 of the synovial fluid versus concentration of power hydrogen ions pH for lipids of the type PC and PS for a constant temperature of 37°C, cartilage wettability We = 40°, average human limbs velocity 1.5m/s, and collagen concentration cc = 500000 mol/mm^3

Rys. A1. Wzrosty dla 0 < pH < 4 oraz spadki dla pH > 4 lepkości dynamicznej cieczy synowialnej ze wzrostem stężenia jonów wodorowych dla molekuł lipidowych typu PC i PS dla ustalonej temperatury człowieka 37°C, przy stałej wodochłonności chrząstki We = 40°, stałym stężeniu włókien kolagenowych cc=500000 mol/mm^3 oraz średniej stałej wartości prędkości 1,5m/s, źródło: badania własne

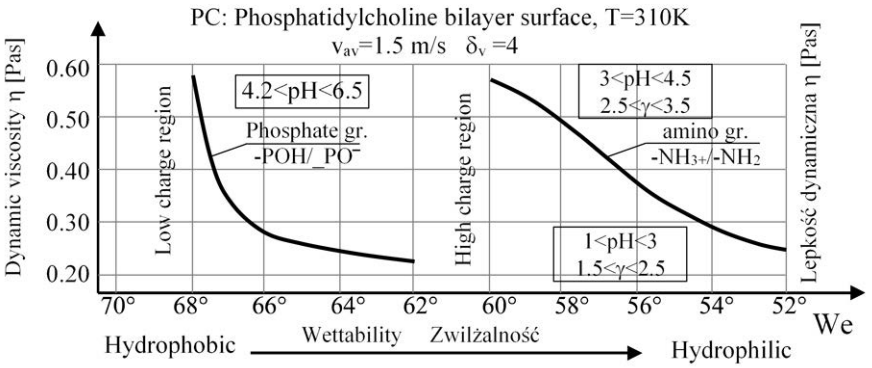

Fig. A2. Dynamic viscosity decrements of the synovial fluid versus cartilage wettability for phospolipids and aminolipids (visible charged surface regions), for a constant temperature of 37°C, constant ranges of pH, average human limbs velocity 1.5m/s, and collagen concentration cc = 500000 mol/mm^3

Rys. A2. Spadki lepkości dynamicznej cieczy synowialnej ze wzrostem wodochłonności We, dla fosfo-i aminolipidów ze wskazaniem obszarów niskiego i wysokiego ładunku elektrostatycznego od PL w temperaturze 37°C, przy ustalonych zakresów pH, stałym stężeniu włókien kolagenowych cc = 500000 mol/mm^3 oraz średniej prędkości 1,5m/s

REFERENCES

1. Taylor, C.J., Dieker, L.E., Miller, K.T., Koh, C.A., Dendy, S.E.: Micromechanical adhesion, Science, 2007, 306, pp. 255–261.
2. Eui-Sung Yoon, Seung Ho Yang, Hung-Gu Han, Hosung Kong: An experimental study on the adhesion at a nano-contact, Wear, 2003, 254, pp. 974–980.
3. De La Fuente, L., Montanes, E., Meng Yizhi, Li Yaxin, Burr, T.J., Hoch, H.C.: Wu Mingming, Assessing adhesion force of Type I and Type IV Pili of Xylella fastidiosa bacteria by use of microfluidic flow chamber, Applied and Environmental Microbiology, 2007, Vol. 73, pp. 2690–2696.
4. Li-Chong Xu, Logan, B.E.: Adhesion forces functionalized latex microspheres and protein-coated surfaces evaluated using colloid probe atomic force microscopy, Colloid and Surfaces B, 48, pp. 84–94, 2006.
5. Manabu Takeuchi: Adhesion Forces of Charged Particles, Chemical Engineering Science, 2006, 61, pp. 2279––2289.

6. Schwender, N., Huber, K., Marravi, F.Al., Hannig, M., Ziegler Ch.: Initial bioadhesion on surfaces in the oral cavity investigated by scanning force microscopy, Applied Surface Science, 2005, 252, pp. 117–122.
7. Wierzcholski K., Miszczak A.: Adhesion Influence on the Oil Velocity and Friction Forces in Conical Microbearing Gap. Scientific Problems of Machines Operation and Maintenance, Polish Academy of Sciences (Zagadnienia Eksploatacji Maszyn Kwartalnik PAN), 2010, z.1(161), Vol. 45, pp. 61–69.
8. Wierzcholski K., Miszczak A.: Adhesion Influence on the Oil Velocity and Friction Forces in Cylindrical Microbearing Gap. Scientific Problems of Machines Operation and Maintenance, Polish Academy of Sciences (Zagadnienia Eksploatacji Maszyn Kwartalnik PAN), 2010, z.1(161), vol. 45, pp. 71–79.
9. Wierzcholski K.: Adhesion and cohesion forces occurring in parabolical microbearing. Tribologia, 2009, 5(227), pp. 221–228.
10. Wierzcholski K.: Adhesion influences on the pressure and carrying capacity of cylindrical microbearing. Tribologia, 2009, 5 (227), pp. 229–236.
11. Wierzcholski K., Miszczak A.: Friction forces on the lubricated surfaces in micro and nanoscale. Journal of Kones Powertrain and Transport, 2008, Vol. 15 No. 4, pp. 597–602.
12. Ziegler B., Wierzcholski K., Miszczak A.: Friction forces measurements by the acoustic emission for slide bearing test stand in University of Applied Science Giessen. Journal of Kones Powertrain and Transport, 2008, Vol. 15 No. 4, pp. 627–633.
13. Ziegler B., Wierzcholski K., Miszczak A.: Friction forces measurements for slide bearing test stand in Maritime University Gdynia using the acoustic emission method. Journal of Kones Powertrain and Transport, 2008, Vol. 15 No. 2, pp. 571–578.
14. Ziegler B., Wierzcholski K., Miszczak A.: Test stand in University of Applied Science Giessen for friction forces measurements in slide bearing using the acoustic emission method. Journal of Kones Powertrain and Transport, 2008, Vol.15 No. 3, pp. 591–595.
15. Ziegler B., Wierzcholski K., Miszczak A.: A new measurements method of friction forces regarding slide journal bearing by using acoustic emission-Continuation.Nowe pomiary sił tarcia w łożyskach ślizgowych przeprowadzone metodą emisji akustycznej-Kontynuacja.Tribologia, 2010, 1(229), pp. 149–156.
16. Ziegler, B., Wierzcholski, K., Miszczak A.: Friction Forces Measurements by the acoustic emission for slide bearing test stand at University of Applied Sciences Giessen, Journal of Kones, 2008, Vol. 15, Nr. 4, pp. 627–633.
17. Silva R.A., Assato M., M.J.S. de Lemos: Mathematical modeling and numerical results of power-law fluid flow over a finite porous medium, International Journal of Thermal Sciences, 2016, Vol. 100, pp. 126–137.
18. Sokolowski M.: Technical Mechanics, Vol. IV Elasticity, PWN, Warsaw 1978.
19. Machado M., Costa J., Seabra E., Flores P.: The effect of the lubricated revolute joint parameters and hydrodynamic force models on the dynamic response of planar multibody systems, Nonlinear Dyn., 2012, Vol. 69, Issue 1, pp. 635–654.
20. Pawlak Z., Urbaniak W., Hagner Derengowska M.: The probable explanation for the low friction of Natural Joints. Cell Biochemistry and Biophysics, 2014, Vol.71, 3, 1615–1621.
21. Pawlak Z., Urbaniak W., Gadomski A., Yusuf K.O., Afara I.O., Oloyede A.: The role of lamellate phospholipid bilayers in lubrication of joints. Acta of Bioengineering and Biomechanics, 2012, Vol. 14, No. 4, pp. 101–106.
22. Wierzcholski K.: Joint cartilage lubrication with phospholipids bilayer. Tribologia, 2016, 2(265), pp. 145–157.